ChemEngineering

MDPI

Communication

One-Stage Aqueous Colloid Process: From the Synthesis of Few-Layer Graphene–PVA Colloids to Efficient Electrospun Nanofibers

Kamel Shoueir, Emeline Lobry, Guy Schlatter and Izabela Janowska *

Institut de Chimie et Procédés pour l'Énergie, l'Environnement et la Santé (ICPEES), CNRS UMR 7515—Université de Strasbourg, 25 rue Becquerel, 67087 Strasbourg, France; rezkshoueir@unistra.fr (K.S.); elobry@unistra.fr (E.L.); guy.schlatter@unistra.fr (G.S.)

* Correspondence: janowskai@unistra.fr

Abstract: Sustainability requirements must be met by the appropriate selection of efficient and environmentally friendly materials and processes. We present materials obtained via all-in-water methods: first, few-layer graphene (FLG)–polyvinyl alcohol (PVA) colloids and then electrospun PVA-FLG fibers. The effects of the FLG concentration, and indirectly of ultrasound, are reflected via the modification of the structural and physical properties, including the microstructure, viscosity, thermal degradation and mechanical properties, of colloids and fiber mats. The primary results are highly encouraging for further optimization and the development of conductive, and mechanically resistant, materials.

Keywords: green process; exfoliation; polyvinyl alcohol nanofibers; PVA–graphene composites; PVA–graphene fibers; electrospinning

Citation: Shoueir, K.; Lobry, E.; Schlatter, G.; Janowska, I. One-Stage Aqueous Colloid Process: From the Synthesis of Few-Layer Graphene–PVA Colloids to Efficient Electrospun Nanofibers. *ChemEngineering* **2024**, *8*, 126. https://doi.org/10.3390/chemengineering8060126

Academic Editor: George Z. Papageorgiou

Received: 9 October 2024
Revised: 15 November 2024
Accepted: 29 November 2024
Published: 9 December 2024

1. Introduction

Polymer nanocomposites are a large and constantly developing family of materials that find applications in many different sectors, according to their properties. Due to the huge recent interest in carbon nanomaterials, especially graphene, intensive research is being carried out on composites containing these nanomaterials. High electrical and thermal conductivity, mechanical strength and flexibility, hydrophobic and barrier characteristics, chemical and thermal resistance, and adsorption are some of the properties that graphene-based nanomaterials can introduce into their composites, particularly in the sectors of energy, medicine, and the environment [1,2].

To benefit from the optimal performances of these composites with nanoscopically related properties at the macroscopic scale, they need to be adequately synthesized/prepared and macronized for final use. The interactions and interface qualities of nanocomposites have a direct impact on the properties of macroscopic composites, being directly related to the final performance. Among the different macroscopic shaping methods, solution electrospinning for 2D shaping seems to be interesting, as it can provide different structures, from nano to microfibers, or morphologies and assemblies with variable surface areas and porosities, consequently finding application in various fields [3]. Filters, membranes, and tissues based on electrospun nanofibers for biomedical applications are of major interest [4].

Despite the diverse potential of electrospinning, the technique requiring an electrostatic field may encounter several significant difficulties in the case of conductive-based material formulations. This is the case for solutions made from carbon nanomaterials. There are several parameters influencing the electrospinning of liquids, which can be defined as "technical" process parameters (voltage, flow rate, type of needle and collector, and distance between them), formulation parameters (concentration, conductivity, molecular weight, surface tension) and environmental conditions [3,5]. As for liquids, solvents with

high volatility and low surface tension maintain a proper balance between the boiling point and evaporation rate. Among the electrospun polymer composites, several examples contain nanocarbon fillers, mainly carbon nanotubes (CNTs) or graphene oxide (GO) [6]. The dispersion of CNTs usually requires the use of surfactants, whereas graphene oxide (GO) is highly hydrophilic and can be dispersed in highly polar solvents such as water. This presence of oxygen-rich hydrophilic groups, which is beneficial to dispersion, deprives GO material of the conductive and mechanical properties associated with the destroyed C=C conjugated lattice [7]. The reason why GO is widely studied is its well-known synthesis by the Hummer method, which, however, has some disadvantages, namely a long duration, harsh oxidation conditions and the need for reduction into reduced GO (rGO) [7,8].

In sustainable development and the circular economy, it is necessary to reduce the number of preparation steps and to use green methods. We recently published a paper on PVA-FLG films, in which FLG was first obtained by exfoliating expanded graphite (EG) in water using bovine serum albumin (BSA) as a surfactant [9,10]. Here, the aqueous PVA-FLG colloid is prepared in situ by the exfoliation of EG in PVA solution (PVA with "surfactant" role) to test the possibility of its direct use for fiber production by electrospinning. The water-soluble PVA polymer, thanks to its biocompatibility and biodegradability, provides an excellent platform for the development of composite materials for various applications, e.g., medical implants, drug delivery systems or food packaging, where the mechanical and gas barrier properties (O_2 for instance) can be tuned using graphene-based additives [11–13]. The thermal and(or) electrical conductivity of such composites open up new application areas.

The challenging aspect of electrospinning is related to the high surface tension of the solvent (i.e., water), a conductive material (FLG), and the lack of surfactant. When it comes to composite solutions such as (PVA + FLG), the nozzle clogging caused by the graphene particles agglomerates is a problem [14]. Here, an annular ring-shaped emitter is used, making the process more efficient and reliable [14].

2. Materials and Methods

PVA (Mowiol, Mw 130,000, Sigma-Aldrich, St-Quentin Fallavier, France) was prepared as a 15 wt.% aqueous solution at 80 °C overnight.

The appropriate amount of expanded graphite (EG, Carbon Lorraine) was added to the PVA solutions and then sonicated for 2 h using an ultrasonicator (BRANSON 550). After exfoliation, the PVA-FLG colloids were subjected to 2 h of settling and then supernatant separation in order to remove the thicker part of weakly exfoliated EG. Three stable aqueous PVA-FLG colloids with 4, 8 and 16 wt. % of FLG were finally obtained.

The electrospinning process was carried out for two hours using a hand-built high-voltage electrospinning machine. The prepared solution was injected into an annular ring-shaped emitter with a 0.5 mm gap and a diameter of 35 mm [14]. The spinning process was controlled with an injection rate of 20 mL/h, voltage of 35 kV, and collection distance of 22 cm. To improve solvent volatilization and the elongation of the fibers, the ambient conditions were carefully maintained in the range of 25–30 °C and the humidity was maintained at 25%.

Scanning electron microscopy (SEM) analysis was performed on the ZEISS Gemini SEM 500 microscope with a resolution of 5 nm.

Diameter distribution histograms were created using the Image J, version 1.5 program.

Transmission electron microscopy (TEM) analyses were performed on the JEOL 2100 FEG microscope operated at 200 kV and equipped with a spherical aberration corrector. Prior to the analysis, the aqueous or ethanol suspension of FLG was transferred by drop casting and then dried onto a classical 300 mesh TEM grid.

Thermogravimetric analyses (TGA) were carried out on TA Instrument Q5000IR by heating the cut electrospun films in the platinum crucibles up to 800 °C with a heating rate of 10 °C/min under an air flow of 25 mL/min.

A rotational rheometer (MCR 301, Anton Paar GmbH) performed the steady-state viscosity measurements of the PVA and PVA-FLG suspensions. The experiments were carried out under R.T. conditions with a cone plate geometry of 50 mm in the shear gap ramp. Viscosity data from 0.1 to 100 s^{-1} were collected to ensure a comprehensive characterization of the rheological behavior of the material.

The mechanical tensile tests on the PVA-FLG nanofiber nonwovens were carried out with a Discovery Hybrid Rheometer DHR 3 from TA Instruments, equipped with linear tensile geometries. Rectangular samples with a width of ~10 mm, a length of ~45 mm and a thickness of ~100 µm were cut from large scaffolds and fixed between two clamps. The thickness of each sample was measured using an IP65 digital micrometer.

3. Results and Discussion

A detailed description of the aqueous PVA colloids containing or not containing FLG is given in the experimental section. It is worth noting that the preparation is a one-step synthesis, first enabling the exfoliation of EG into FLG by PVA "surfactant-like" action under ultrasonication into the well dispersed PVA-FLG colloids and then their electrospinning. Three composites were obtained, with relative weight FLG contents of 4, 8 and 16% according to TGA analysis, as described below. An optical image of the representative macroscopic electrospun fiber sheets is presented in Figure 1.

Figure 1. Optical image of electrospun fiber sheets: PVA-FLG (16%) on the left, PVA on the right, inset: PVA-FLG (4%).

According to the SEM micrographs, the electrospun materials are an assembly of smooth fibers with an average lateral diameter of about 0.1 to 0.6 µm, as shown in Figure 2. A more detailed distribution is presented on the histograms collected from the average resolution micrographs (10 µm scale), as shown in Figure 2. There is no clear correlation between the FLG concentration and fiber diameter, as observed for the CNT fillers in polyacrylonitrile [15]. The average diameter of fibers decreases from 0.36 µm for PVA to 0.22 µm and 0.23 µm for PVA-FLG (4%) and (8%), and increases to 0.4 µm for PVA-FLG (16%). This phenomenon can be explained by the viscosity differences, as shown below, and by the steric expansion effect in the case of most FLG-charged composites. For the composites with a lower FLG content (4, 8%) and especially in PVA-FLG (4%), the fiber diameter is more homogenous compared to that in PVA fibers. Due to the relatively large lateral size of the FLG flakes, the flakes can be easily distinguished from the overall fiber morphology. They are either individually embedded/integrated into the PVA fiber, mainly in the case of smaller FLG flakes (Figure 2, PVA-FLG (8%) and PVA-FLG (16%), high resolution), or provide a platform for fiber interconnections (Figure 2, PVA-FLG (4%), medium and high resolution, PVA-FLG (16%), low and medium resolution). In both cases, they are well covered by PVA, which confirms the good interface between both species.

This compatibility is particularly observed in the PVA-FLG (4%) film, where a kind of glued network is formed.

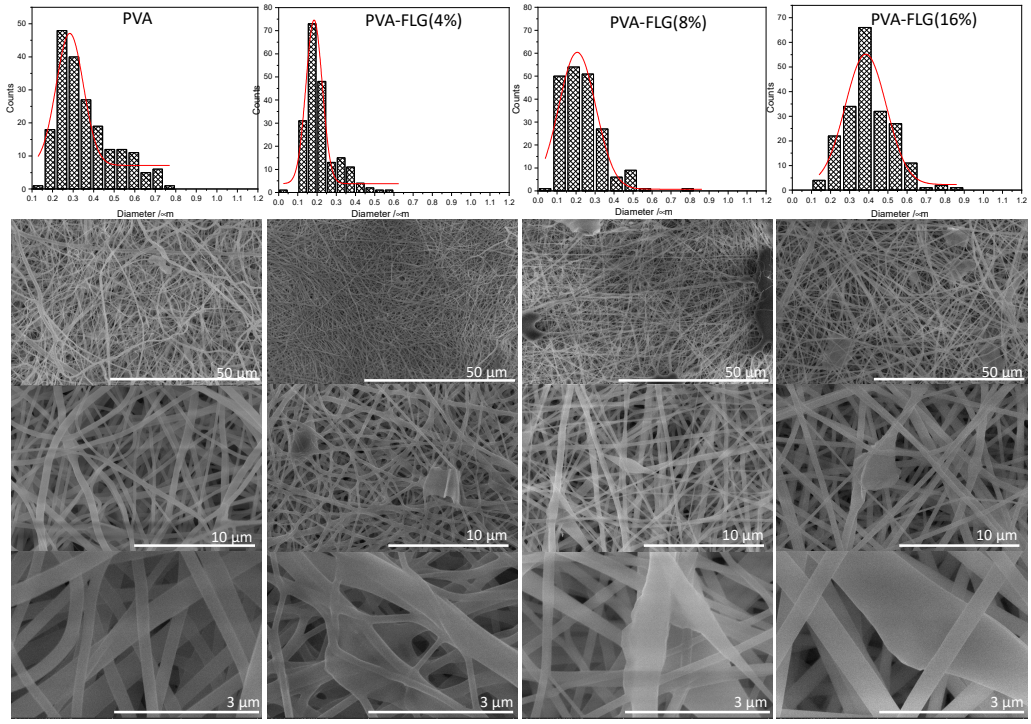

Figure 2. Diameter distribution and SEM micrographs of PVA and PVA-FLG nanofibers (PVA, PVA-FLG (4%), PVA-FLG (8%), PVA-FLG (16%). For pristine PVA fibers (i.e., left column), the solution was not sonicated.

Compared to pristine PVA fibers prepared from a non-sonicated solution (Figure 2, left column), additional SEM micrographs (Figure 3) revealed that the ultrasonication treatment increased the uniformity of the PVA fibers (named after PVA–sonic fibers), which had a mean diameter of 0. 44 µm. This indicates that ultrasound has a beneficial effect on the solubilization and homogeneity of PVA in water, which could originate from a different chain entanglement. Similar findings were observed by Shenoy et al., who investigated the self-interactions of PVA solutions prepared at 80 °C and 92 °C [16].

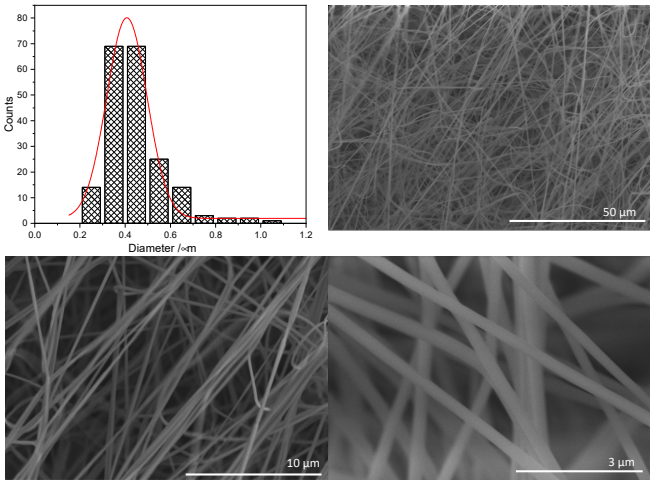

Figure 3. Diameter distribution and SEM micrographs of PVA fibers with different resolutions prepared from a sonicated solution.

The highly developed interface between PVA and FLG flakes could be observed via TEM, as shown in Figure 4a–c. Due to the covering by the polymer, a deeper analysis of the FLG surface and edges in order to determine the number of sheets in a single FLG flake is challenging. To solve this issue, the prolonged acquisition was applied directly to the surface of the composites to expose the highly graphitic FLG surface, as shown in Figure 4c. To count the number of sheets, the combustion of the composite at 500 °C was performed prior to the analysis. Data from several micrographs confirm a variable number of sheets, mostly lower than 10, as shown in Figure 4a–f. The results are very promising, as a lower number of FLG sheets could be achieved via the optimization of the synthesis parameters.

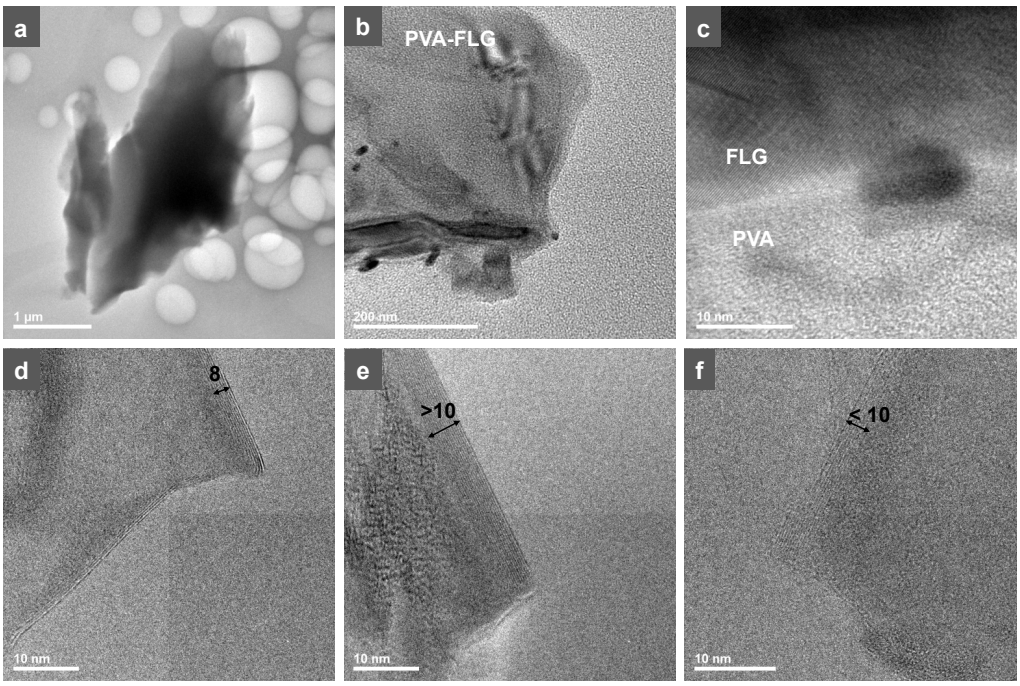

Figure 4. TEM micrographs: (**a**,**b**) PVA-FLG composite, (**c**) PVA-FLG composite after prolonged electron exposition, (**d**–**f**) FLG flakes from PVA-FLG after combustion at 500 °C.

The TGA combustion curves above 530 °C clearly show the presence of FLG in the fibers, with the relative amount of FLG reaching around 4, 8 and 16%, Figure 5. Above this temperature, the combustion of pure PLA is complete.

The first combustion zone up to c.a. 250 °C, often related to physiosorbed species such as water, changes slightly from a dropping one by c.a. 8% wt (%) for pure PVA to quasi-stable PVA or even increasing one in the case of the composites. In DTG, there are three clearly distinguishable peak maxima, which shift downwards or upwards by 20–30 °C depending on the FLG content. Detailed analysis shows some shifts in T_{onset} and T_{offset} up to 20° and 40 °C, respectively. In general, the main combustion zone ($T_{offset} - T_{onset}$) is narrower in the composites by about 20 °C compared to PVA, without taking into account the last combustion zone related to the remaining FLG. In PVA-FLG (4%) and PVA-FLG (16%), a higher temperature is required for the combustion of wt. 50% (T_{50}) compared to pure PVA, i.e., 420 °C vs. 380 °C, and then the combustion accelerates in the higher temperature zones. These modifications may be related to the formation of a physical barrier at FLG and the problem of the diffusion of degraded PVA gas species [17], and on the other hand, the high thermal conductivity of FLG, which causes faster heat transfer and the accelerated interfacial degradation of PVA [9]. The effect of ultrasounds can be observed in the TGA of PVA–sonic fibers compared to non-sonicated PVA. The main changes include the quasi-absence of adsorbed species in the low-temperature region and the overall combustion running faster, especially in the first main zone ($T_{offset} - T_{onset}$ = 260 °C instead of 340 °C in PVA). Here, 50 wt.% of PVA–sonic was already oxidized at T_{50} = 345 °C instead of 380

°C for PVA. The behavior of PVA–sonic fibers under oxidative TGA conditions is consistent with SEM observations confirming a kind of homogenization of PVA chains through their lower entanglement, or shortening (or both). The shortening of PVA chains eventually caused by the tip-ultrasonications may be related to the cavitation and sonolysis process occurring during ultrasonication in water [18,19]. Acoustic cavitation in the presence of air generates hydrogen, hydroxyl radicals and superoxide radicals that can attack the polymer chains. In the composites, the additional role of EG or FLG during the ultrasonication is difficult to assess in this context. The high thermal conductivity of the nanocarbons and their potential radical scavenging have to be taken into account; therefore, the further shortening and functionalization of PVA chains cannot be excluded [20].

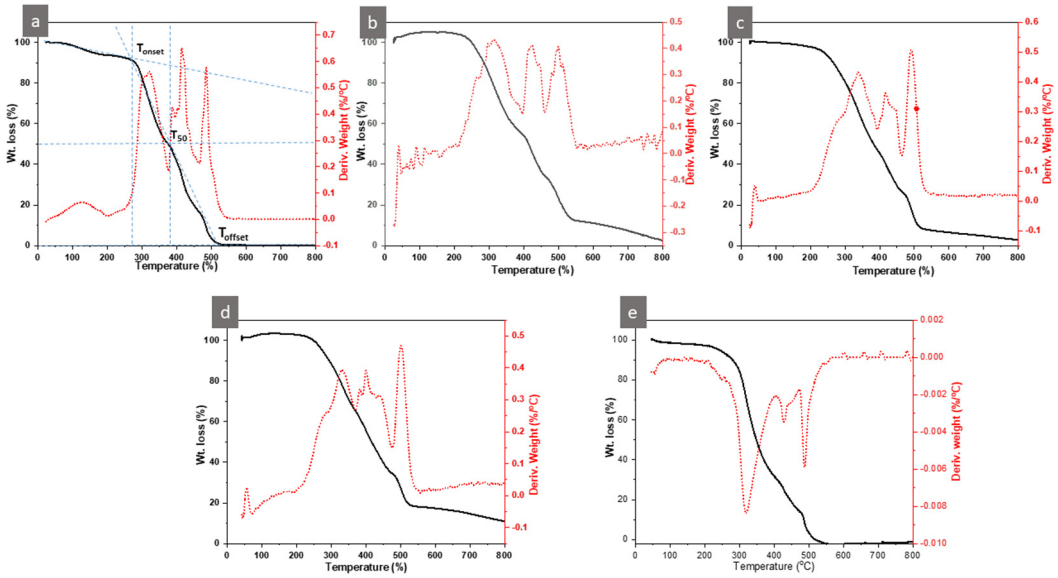

Figure 5. TGA (and DTG) analysis curves of PVA (**a**), PVA-FLG (**b**–**d**) composites, and PVA–sonic (**e**).

According to rheology, as shown in Figure 6a, the viscosity of pure PVA colloid remains almost unchanged after ultrasonic treatment, indicating that the modification of the polymer chains observed via TGA and SEM microscopy does not have a significant effect on the viscosity. As for the composites, the viscosity decreases in PVA-FLG (4%) and PVA-FLG (8%), which is not related to the addition of FLG but to the decantation process that follows the sonication treatment. As described above, due to the decantation step applied in order to settle and remove the thicker part of FLG, well-stabilized supernatant suspensions with a lower FLG concentration are recovered. The lower viscosity of the supernatants compared to PVA alone indicates that a part of the PVA settled down together with FLG, confirming the PVA–FLG interactions. With the subsequent stepwise addition of FLG, the viscosity increases, with the most concentrated sample almost reaching the same value as that for pure PVA. To check the impact of the decantation step, viscosity measurements were also performed for the non-stabilized colloid (without decantation). As expected, the viscosity of such a composite is significantly higher than that of PVA alone. The change in viscosity in the presence of FLG is an important factor that needs to be optimized in the subsequent electrospinning process.

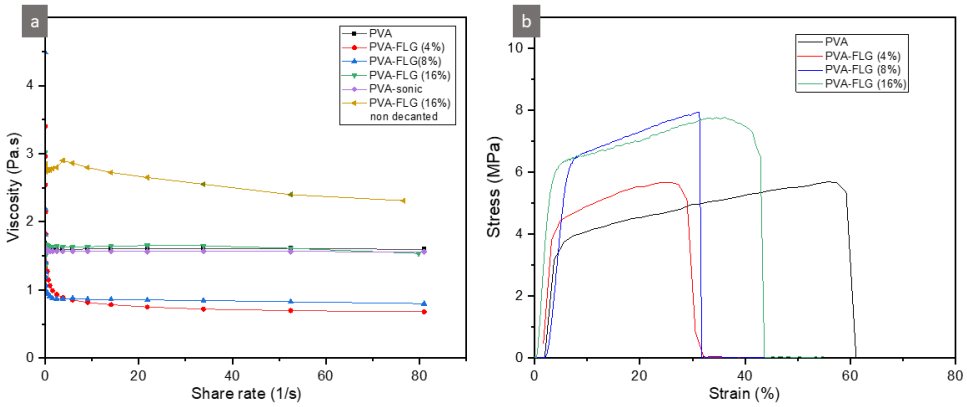

Figure 6. (**a**) Viscosity vs. shear rate curves of PVA, PVA-FLG composites, PVA–sonic, and PVA-FLG (16%) non-decanted; (**b**) stress–strain curves for PVA and PVA-FLG composites.

The basic properties of electrospun fibers, such as electrical conductivity and mechanical resistance, were investigated. As can be observed in Figure 6b, the addition of FLG affects the mechanical properties, and in general the composites exhibit a higher tensile modulus and tensile strength, with decreased ductility compared to PVA alone. The increase in the FLG content from 4 to 8 wt.% results in an increased tensile strength without significantly modifying the ductility, while further loading with FLG up to 16 wt. % has a negligible effect on the tensile strength with the increase in elongation at break. Due to the relatively high thickness of FLG flakes at this stage of development, the FLG content, ensuring the notable improvement of the mechanical properties in the composites, is much higher than that of the composites containing rGO [8,21]. As mentioned above, the most significant advantage lies in the preparation method, which avoids the harsh conditions needed to provide GO first (strong oxidants) and then rGO (e.g., hydrazine, temperature ≈ 1000 °C). The improvement in mechanical performance is similar to that recently reported for a multilayer film made from electrospun PVA fibers coated with electrosprayed rGO flakes and then hot-pressed (22 MPa tensile strength and 34% elongation at break, 13.7% rGO) [16]. The optimal results obtained here for the most charged composite show that the FLG amount could be increased further. Higher FLG loading would also ensure the conductivity of the films. In this context, the associated interconnected organization of FLG with the fibers observed locally via SEM is also encouraging. The prepared fiber films are not yet conductive even at the highest FLG loading, which is primarily attributed to the intrinsic properties of FLG due to its still considerable thickness and/or the insufficiently favorable distribution and arrangement of FLG inside the fibers and of the fibers themselves. The phenomena of percolation are more complex than in the case of previously studied drop-cast PVA-FLG films. The different structure of the components in the films produced using both techniques makes them hardly comparable [9]. In drop-casted films, the optimal mechanical improvement was observed for the composite containing 1%wt. FLG, while charge percolation occurred at a loading of 3% wt.

4. Conclusions

The initial experiments involving the direct synthesis of FLG via the exfoliation of EG in water with PVA to FLG-PVA colloids, followed by the efficient electrospinning of the colloids into nanofibers films, show very promising results. Further optimization concerns several parameters related to colloid synthesis (in order to obtain thinner FLG flakes) and electrospinning. Regardless of the conductivity requirements, the presented engineering concept may also be useful in other application areas, such as the medical sector and the use of implants with enhanced mechanical properties.

Author Contributions: Conceptualization, K.S. and I.J.; methodology, all authors; software, K.S.; validation, I.J. and G.S.; formal analysis, K.S.; investigation, K.S.; resources, I.J. and G.S.; data curation, K.S.; writing—original draft preparation, I.J.; writing—review and editing, I.J.; visualization, K.S. and I.J.; supervision, I.J., E.L. and G.S.; project administration, I.J.; funding acquisition, K.S. and I.J. All authors have read and agreed to the published version of the manuscript.

Funding: This research received no external funding.

Data Availability Statement: The raw data supporting the conclusions of this article will be made available by the authors on request.

Acknowledgments: Walid Baazis from IPCMS is acknowledged for performing the TEM microscopy. Thierry Romero is acknowledged for carrying out the SEM microscopy.

Conflicts of Interest: The authors declare no conflicts of interest.

References

1. Zhu, P.; Yan, Y.; Zhou, Y.; Qi, Z.; Li, Y.; Chen, C.-M. Thermal Properties of Graphene and Graphene-Based Nanocomposites: A Review. *ACS Appl. Nano Mater.* **2024**, *7*, 8445–8463. [CrossRef]
2. Ma, Y.; Bai, D.; Hu, X.; Ren, N.; Gao, W.; Chen, S.; Chen, H.; Lu, Y.; Li, J.; Bai, Y. Robust and antibacterial polymer/mechanically exfoliated graphene nanocomposite fibers for biomedical applications. *ACS Appl. Mater. Interfaces* **2018**, *10*, 3002–3010. [CrossRef] [PubMed]
3. Ahmadi Bonakdar, M.; Rodrigue, D. Electrospinning: Processes, structures, and materials. *Macromolecules* **2024**, *4*, 58–103. [CrossRef]
4. Xue, J.; Wu, T.; Dai, Y.; Xia, Y. Electrospinning and electrospun nanofibers: Methods, materials, and applications. *Chem. Rev.* **2019**, *119*, 5298–5415. [CrossRef]
5. Mailley, D.; Hébraud, A.; Schlatter, G. A Review on the Impact of Humidity during Electrospinning: From the Nanofiber Structure Engineering to the Applications. *Macromol. Mater. Eng.* **2021**, *306*, 2100115. [CrossRef]
6. Wang, C.; Li, Y.; Ding, G.; Xie, X.; Jiang, M. Preparation and characterization of graphene oxide/poly (vinyl alcohol) composite nanofibers via electrospinning. *J. Appl. Polym. Sci.* **2013**, *127*, 3026–3032. [CrossRef]
7. Yu, H.; Zhang, B.; Bulin, C.; Li, R.; Xing, R. High-efficient synthesis of graphene oxide based on improved hummers method. *Sci. Rep.* **2016**, *6*, 36143. [CrossRef]
8. Bao, C.; Guo, Y.; Song, L.; Hu, Y. Poly(vinyl alcohol) nanocomposites based on graphene and graphite oxide: A comparative investigation of property and mechanism. *J. Mater. Chem.* **2011**, *21*, 13942–13950. [CrossRef]
9. Van der Schueren, B.; El Marouazi, H.; Mohanty, A.; Lévêque, P.; Sutter, C.; Romero, T.; Janowska, I. Polyvinyl alcohol-few layer graphene composite films prepared from aqueous colloids. Investigations of mechanical, conductive and gas barrier properties. *Nanomaterials* **2020**, *10*, 858. [CrossRef]
10. Ba, H.; Truong-Phuoc, L.; Pham-Huu, C.; Luo, W.; Baaziz, W.; Romero, T.; Janowska, I. Colloid approach to the sustainable top-down synthesis of layered materials. *ACS Omega* **2017**, *2*, 8610–8617. [CrossRef]
11. Sobhiga, G.; Maria, H.J.; Mozetič, M.; Thomas, S. A review on green materials: Exploring the potential of poly(vinyl alcohol) (PVA) and nanocellulose composites. *Int. J. Biol. Macromol.* **2024**, *283*, 137176. [CrossRef] [PubMed]
12. Aslam, M.; Kalyar, M.A.; Raza, Z. Polyvinyl alcohol: A review of research status and use of polyvinyl alcohol based nanocomposites. *Polym. Eng. Sci.* **2018**, *58*, 2119–2132. [CrossRef]
13. Baker, M.I.; Walsh, S.P.; Schwartz, Z.; Boyan, B.D. A review of polyvinyl alcohol and its uses in cartilage and orthopedic applications. *J. Biomed. Mater. Res. B Appl. Biomater.* **2012**, *100*, 1451–1457. [CrossRef]
14. Dodero, A.; Castellano, M.; Vicini, S.; Hébraud, A.; Lobry, E.; Nhut, J.; Schlatter, G. Eco-Friendly Needleless Electrospinning and Tannic Acid Functionalization of Polyurethane Nanofibers with Tunable Wettability and Mechanical Performances. *Macromol. Mater. Eng.* **2022**, *307*, 2100823. [CrossRef]
15. Heikkilä, P.; Harlin, A. Electrospinning of polyacrylonitrile (PAN) solution: Effect of conductive additive and filler on the process. *Express Polym. Lett.* **2009**, *3*, 437–445. [CrossRef]
16. Shenoy, S.L.; Bates, W.D.; Wnek, G. Correlations between electrospinnability and physical gelation. *Polymer* **2005**, *46*, 8990–9004. [CrossRef]
17. Patole, A.S.; Patole, S.P.; Jung, S.-Y.; Yoo, J.-B.; An, J.-H.; Kim, T.-H. Self assembled graphene/carbon nanotube/polystyrene hybrid nanocomposite by in situ microemulsion polymerization. *Eur. Polym. J.* **2012**, *48*, 252–259. [CrossRef]
18. Flint, E.B.; Suslick, K.S. The temperature of cavitation. *Science* **1991**, *253*, 1397–1399. [CrossRef]
19. Suslick, K.S. Sonochemistry. *Science* **1990**, *247*, 1439–1445. [CrossRef]

20. Yang, H.; Xu, S.; Jiang, L.; Dan, Y. Thermal decomposition behavior of poly (vinyl alcohol) with different hydroxyl content. *J. Macromol. Sci. Part B* **2012**, *51*, 464–480. [CrossRef]
21. Ghobadi, S.; Sadighikia, S.; Papila, M.; Cebeci, F.Ç.; Gürsel, S.A. Graphene-reinforced poly(vinyl alcohol) electrospun fibers as building blocks for high performance nanocomposites. *RSC Adv.* **2015**, *5*, 85009–85018. [CrossRef]